Scientific Research Publishing

Voice of the Publisher, 2025, 11(3), 538-556
https://www.scirp.org/journal/vp
ISSN Online: 2380-7598
ISSN Print: 2380-7571

Spatial-Temporal Assessment of Gaseous and Particulate Matter Pollutants during COVID-19 Lockdown over Kenya, East Africa

Peter M. Mutama[1], John W. Makokha[1], Festus B. Kelonye[2], Geoffrey W. Khamala[1]

[1]Department of Science, Technology and Engineering, Kibabii University, Bungoma, Kenya
[2]Department of Biological and Environmental Science, Kibabii University, Bungoma, Kenya
Email: makokhajw@gmail.com

How to cite this paper: Mutama, P. M., Makokha, J. W., Kelonye, F. B., & Khamala, G. W. (2025). Spatial-Temporal Assessment of Gaseous and Particulate Matter Pollutants during COVID-19 Lockdown over Kenya, East Africa. *Voice of the Publisher, 11,* 538-556.
https://doi.org/10.4236/vp.2025.113036

Received: June 13, 2025
Accepted: September 13, 2025
Published: September 16, 2025

Abstract

Varied naturally occurring and anthropogenic emissions within the Kenyan territory contribute to elevation of levels of organic and inorganic, gaseous and particulate pollutant types. A study to ascertain main contributing factors to the status quo was vital. The study compares satellite-derived datasets for five main pollutant parameters, such as Black carbon (BC), Sulphur Dioxide (SO_2), Nitrogen Dioxide (NO_2), Carbon Monoxide (CO), and Ozone gas (O_3) for three equal periods: pre-lockdown (April-June 2019), lockdown (April-June 2020) and post-lockdown (April-June 2021). The study utilized Aura/Ozone Monitoring Instrument (OMI), Modern-Era Retrospective analysis for Research and Applications version 2 (MERRA-2), and MODIS (Moderate-resolution Imaging Spectroradiometer) satellite sensors to ascertain the variations in anthropogenic emissions into the atmosphere during COVID-19 lockdowns in Kenya. This was achieved by doing a phase-wise analysis of spatial-temporal variation of the fore mentioned five main pollutants over Kenya during the pre, during and post lockdown phases. The datasets obtained were manipulated using the Adobe Illustrator (2015 series) and the Grid Analysis and Display System (Grads) Version 2.2.1.oga.1 for the above-mentioned pollutants from 2019 to 2021 (April-June). It was evident that the spatial-temporal variability of the pollutants did not depict a significant reduction in the lockdown phase. This was because of the migration of aerosols from regional sources, the dominance of natural sources such as geothermal activities, and low stringent levels of lockdown protocols. However, meteorological factors had a great influence on the variability of the concentration of pollutants over the sampled region with the MAM (March-April-May), considered wet, season recording lower concentrations and JJA (June-July-August), considered a dry season, registering the highest concentrations.

Keywords

Air Quality, COVID-19, Lockdowns, Pollution

1. Introduction

Severe Acute Respiratory Syndrome (SARS) virus has been named Corona Virus Disease 2019 (COVID-19) (World Health Organization, 2020) whose symptoms are related to the already witnessed SARS and Middle East Respiratory Syndrome (MERS) virus (Lukiw et al., 2022). Covid-19 virus had infected over 2.95 million people globally and killed 1931000 people by March 2020 (Bai et al., 2022). The pandemic has been a highly disruptive event (Wong et al., 2021). Lockdowns instituted to control the spread of the COVID-19 virus, has had unforeseen decrease in economic and social activities and the associated emission of air pollutants and greenhouse gases worldwide (Kumar et al., 2022). This episode provides a rare opportunity to the scientific world to detect and understand the impact of anthropogenic emissions on Earth's atmosphere at all spatial scales, from region to global (Monsen, 2024). Particular interest in this study is focused on the changes that this COVID-19 lockdowns will have on the ambient concentrations of inhalable Particulate Matter (PM) suspended in air, Nitrogen Dioxide (NO_2), Sulphur Dioxide (SO_2), Carbon Monoxide (CO) and ozone gas (O_3). Airborne particulate matter (PM) is a major environmental risk factor with adequately documented short-term (Hassan et al., 2022) and long-term effects on both human morbidity and mortality (Ferranti et al., 2017; Gkatzelis et al., 2021). Long-term effects of exposure to air pollution include asthma, chronic obstructive pulmonary disease (COPD), pulmonary fibrosis, cancer, type 2 diabetes, and other diseases (Gupta et al., 2020). There is high correlation between type of PM to the extent of health impacts, with P.M of aerodynamic diameter less than 2.5 μm typically having more significant health implications on humans (Halmer et al., 2002). Nitrogen dioxide (NO_2) is a highly reactive pollutant emitted mainly from fossil fuel combustion. Traffic pollution is considered as a major source of NO_2 emissions (Carslaw, 2005). Levels of NO_2 are observed to decay with increasing distance from main expressways declining to background levels by 300 meter (Khan & Siddiqui, 2014). Carbon Monoxide (CO) is mainly formed in industries and engines, where it is a product of the incomplete combustion of fuels (Kumar et al., 2007). Once it is inhaled, it reacts with the blood's oxygen and causes harm to the organs, particularly the heart and brain, whereas a high concentration of this gas is deadly (Kumar, 2017). Sulphur dioxide is a colorless gas with a sharp, irritating odour produced by burning fossil fuels and by smelting of mineral ores that contain Sulphur (Levelt et al., 2006). Erupting volcanoes can be a significant natural source of Sulphur Dioxide emissions (Lippi et al., 2012). When Sulphur dioxide combines with water and air it forms sulphuric acid, which is a main component of acid rain (Kumar et al., 2007).

Acid rain can cause deforestation, corrode roofing materials and paints, and acidify water to the detriment of aquatic life (Meng et al., 2013). Sulphur dioxide affects the respiratory system, particularly lung function, and can irritate eyes (Pant & Harrison, 2013). It causes coughing, mucus secretion and aggravates conditions such as asthma and chronic bronchitis (Venter et al., 2020). Ozone gas comprises three oxygen atoms, a pair of which forms normal oxygen, and a single attached to the molecule making it an unstable gas. This gas is naturally found among the atmosphere layers, between the troposphere and stratosphere, and contributes immensely to protecting human beings from the ultraviolet radiation (UV) received from the sun. However, the layer-ozone is produced from the reaction of industrial and transportation facilities discharges with sunlight, and it could transfer far away from the main source (World Health Organization, 2006). Ozone gas (O_3) is an example of a secondary pollutant species formed exclusively through atmospheric chemical reactions. Pollutants that are the raw materials for the formation of O_3 are nitrogen oxides (NO_x), volatile organic compounds (VOCs), Sulphur dioxide (SO_2), carbon monoxide (CO) and ammonia (NH_3) (De et al., 2018). The main environmental phenomenon in Kenya is vehicular exhaust, biomass burning, and dust from the dry northern and northeastern regions. Back trajectory analysis by (Misiani et al., 2019) showed that aerosols mainly dust and sea salt reaching Kenya were transported from either Arabian or Indian sub-content or western parts of the Indian Ocean respectively. The Sahara Desert is also considered as a source of mineral aerosols (Laurent et al., 2008). On the regional level (Otmani et al., 2020) researched on the contribution of COVID-19 lockdowns on reducing the ambient concentration of NO_2, PM_{10} and SO_2, over Sale city, Morocco. In his context, measurement of NO_2, SO_2, and PM_{10}, was done pre and during COVID-19 lockdown phase. The results obtained indicated that the difference between the concentrations obtained before and after lockdowns were 96%, 49%, and 75% for, SO_2, NO_2 and PM_{10} respectively. A study to simulate the relationship between lockdowns and air quality and variation in pollutant concentrations has not been done in East Africa. A review of the literature indicates that several studies have been done worldwide on this area of study, however, in the studies; no empirical link has been established between lockdowns and changes in air quality. The impact of the lockdowns and curfews on the environment may be temporary and not significant but governments and individuals can learn from these lockdown measures on how to reduce pollution on a long-term basis (Arora et al., 2020). The government protocols for the COVID-19 virus pandemic have had a considerable effect on pollutant concentrations in the atmosphere.

2. Study Site

Kenya is a country in the East Africa region located between the longitudes 32˚ East and 42˚East and latitudes 5˚ South and 5˚ North. It is bordered by Ethiopia to the north, Tanzania to the south, South Sudan to the northwest, Uganda to the

west, and Somalia to the east (Khadiagala, 2010) as shown in **Figure 1**. The country is populous with a population of 47,564,296 according to the demographic survey of Kenya 2019 (Karambu et al., 2024).

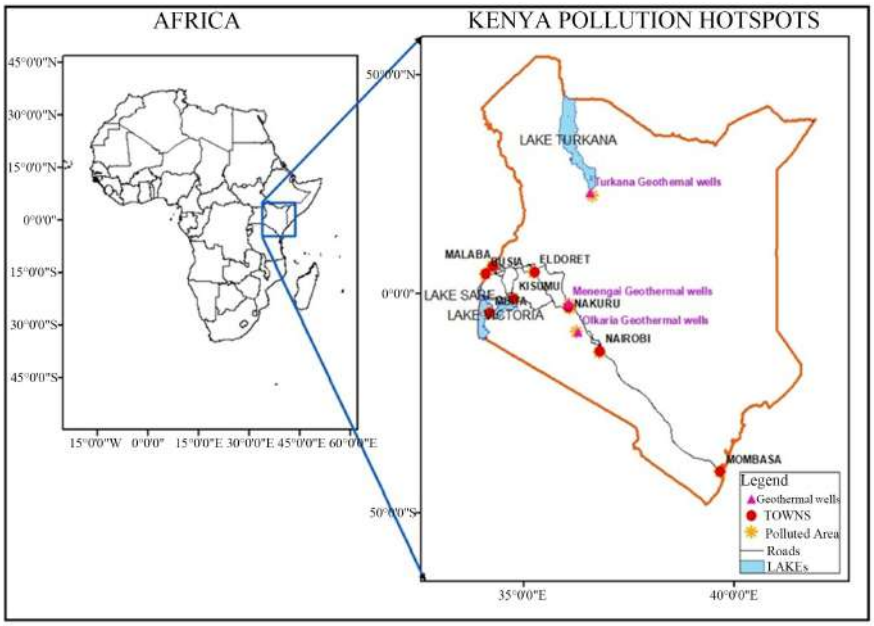

Figure 1. Map of Kenya.

Kenya has a land area of about 56937 km^2 with varying topography which includes glaciated mountain peaks with permanent snow cover, plateaus, and coastal plain (Worldmeter, 2025). The country has a rift valley lying midway across the territory, which splits it into the western part that slopes down to Lake Victoria from Mau ranges and Mount Elgon (4300 m) and the eastern part which is dominated by Mount Kenya (5200 m) and the Aberdare ranges (altitude 4000 m).The long-term annual average values of temperature over the Kenyan territory are 25˚C to 34˚C while the relative humidity ranges between 24.0% and 69.0% respectively (Ndolo, 2018). This region is a high precipitation region except the north and northeastern regions and records a total of between 200 mm and 600mm rainfall in a year. The weather condition in Kenya is generally humid (Obiero & Onyando, 2013).

3. Data and Methods

3.1. Air Quality Data and Study Period

The part of the air quality data to be discussed in the proposed research is to be obtained from the MERRA-2 model on board the MODIS satellite and MERRA-2 model. This will include daily concentration. Spatial maps and time series of particulate matter of aerodynamic diameter of 10 μm and 2.5 μm, Nitrogen Dioxide, carbon monoxide, Sulphur Dioxide and Ozone gas carbon monoxide are accessible through retrievals from both satellite sensors and models.

To ascertain the impact of lockdown on air quality, the study is done in three

phases as designed by Mahato et al. (2020) as follows:

1) Pre-lockdown—April 1st to June 30th 2019.

2) During Lockdown—April 1st to June 30th 2020.

3) Post-lockdown—April 1st to June 30th 2021.

These data ranges were selected in such a way as to correspond to the lockdown phase instituted by the government of Kenya in the year 2020. The justification of the Mahato et al. (2020) design is based on the fact that periods further away from the lockdown period would introduce inaccuracies in making comparison of the pollution concentrations as a result of contribution of other environmental episodes apart from lockdowns.

3.2. Instrumentation

3.2.1. Moderate Resolution Imaging Spectroradiometer (MODIS)

MODIS aboard both NASA's Terra and Aqua satellites is a sensor with the ability to characterize the spatial and temporal characteristics of the global aerosol field (Mutama et al., 2024). Launched in December 1999 and May 2002, MODIS has 36 channels spanning the spectral range from 0.44 to 15 μm. These measurements are used to derive spectral aerosol optical thickness and aerosol size parameters over both land and ocean (Mutama et al., 2024; Li et al., 2003). MODIS aerosol retrievals co-located with AERONET measurements confirm that one-standard deviation of MODIS optical thickness retrievals falls within the predicted uncertainty of $\Delta\tau = \pm 0.03 \pm 0.05\tau$ over ocean and $\Delta\tau = \pm 0.03 \pm 0.15\tau$ over land (Li et al., 2003). The images of retrievals at the global scale are constructed from the aerosol optical thickness and size parameter products derived from observed MODIS radiances. Red indicates aerosol dominated by small particles (less than 0.5 μm) and greenish tints indicate aerosol with a higher proportion of large particles (greater than 0.5 μm). Thus, MODIS can be used to separate aerosols by size, an ability that can be used as a proxy for separating anthropogenic aerosols from natural sources, and increase the accuracy of estimating human induced aerosol forcing (Remer et al., 2005).

3.2.2. Ozone Monitoring Instrument (OMI)

The Ozone Monitoring Instrument on board the Aura satellite provides high-resolution data sets with daily global coverage (Khamala et al., 2022). The instrument measures a reflectance in wavelength 264 - 504 nm. The Absorbing Aerosol Optical Depth (AOD) used in this study is retrieved using OMAERUV algorithm, which is explained in (Makokha et al., 2017; Boiyo et al., 2017). OMI is a portable instrument on Aura for monitoring the recovery of the ozone in response to the phase out of chemicals (Levelt et al., 2018). Datasets for the ground-based concentrations of the greenhouse gases was obtained from the OMI online platform. The level −3 AOD at $1^\circ \times 1^\circ$ grid resolution is available from the NASA Goddard Earth sciences, Data and Information Services Centre (GESDISC; https://disc.sci.gsfc.nasa.gov).

3.3. Modern-Era Retrospective Analysis for Research and Applications, Version 2 (MERRA-2)

MERRA-2 provides data starting from 1980. It was introduced as a replacement for the original MERRA dataset because it was more advanced made in the assimilation system that enables the assimilation of modern hyper spectral radiance and microwave observations, along with GPS-Radio-Occultation datasets. It also uses NASA's Ozone layer profile observations that began in late 2004. MERRA-2 is the first long-term global reanalysis to assimilate the space-based observations of aerosols and represent their interactions with other physical processes in the climate system. The MERRA-2 plat form provided datasets for combined dark blue AOD at $\lambda = 500$ nm, AE at $\lambda = 440$ nm, and SSA. The primary data of pollutants concentrations were cross-referenced with the satellite image through spatial and temporal analysis of the pollutants. The satellite images were procured from the open access platform from NASA, which is officially available as "NASA GIOVANNI V4.34". The data obtained were manipulated with the aid of Adobe Illustrator (2015 series) and Grid Analysis and Display System (Grads) Version 2.2.1.oga.1 (Copyright 1988-2018 by George Mason University) for the above-mentioned pollutants for the period of 2017 to 2020 (April - June). The spatial distribution of each pollutant was obtained and specified for our area of interest. Different atmospheric pollutants (CO, NO_2, O_3, BC, and SO_2) were collected from satellite data from 2017 to 2020 for Nairobi, Mombasa and Kisumu Cities. The data accessed from the GIOVANNI (Goddard Earth Sciences Data and Information Services Centre, or GES DISC), indicates various Geoscience data from NASA satellites directly on the web portal (https://earthdata.nasa.gov/), instead of the cumbersome traditional data acquisition and analysis methods. The pollutants CO, SO_2, and BC were obtained from the source MERRA-2 model (GMAO 2015) and NO_2, and O_3 from the source OMDOAO3e (Cheng et al., 2021) with a spatial resolution of 0.25˚. The data were available as net-CDF files obtained data as a net-CDF file, which can be opened in the Grads software, and further, the data was displayed as Jpeg format images.

4. Results and Discussions

Changes in the concentration of Particulate Matter (PM) and Greenhouse Gases After the declaration of lockdowns starting on 22nd March 2020, pollution of the atmosphere worldwide and in the region witnessed a substantial reduction (De et al., 2018). Especially, during the study period anthropogenic black inorganic carbon, nitrogen dioxide, carbon monoxide, Sulphur dioxide has shown marginal declining trends (De et al., 2018). Time average maps of daily concentrations of these pollutants have shown major changes in their display which depicted reduced concentration of the pollutants. Western Kenya, the region around Nakuru, and parts of Turkana County did register though not significant relatively higher concentrations of black inorganic carbon, nitrogen dioxide, carbon monoxide, and Sulphur dioxide.

4.1. Inorganic Black Carbon

Figure 2 shows BC composites over Kenya for pre-lockdown, lockdown, and post-lockdown for a similar period in 2019 to 2020. There was a significant decrease in BC concentrations during April, May, and June in 2020. Though there is an effect of downwash because of high precipitation, the drop is sharper and high in 2020 because of the lockdown and curfews in all the regions.

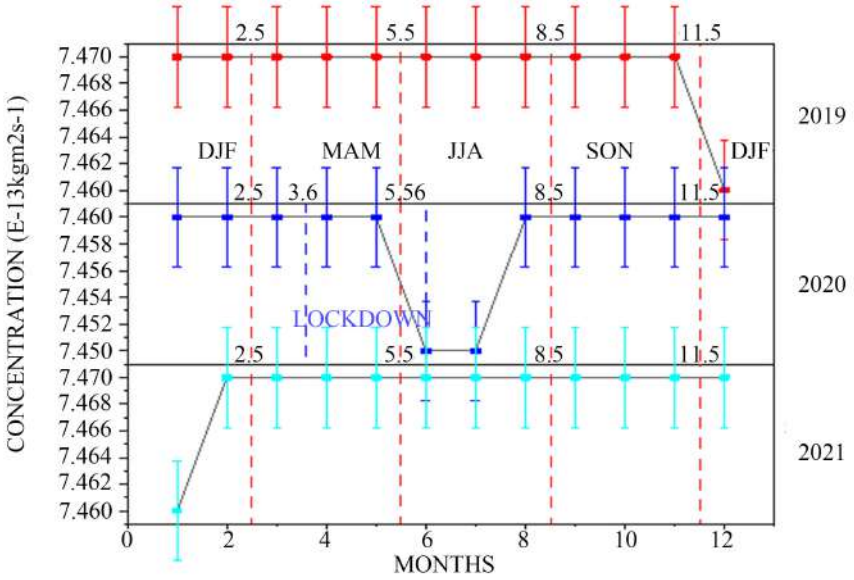

Figure 2. Time series, total area-average of surface mass concentration of daily concentration of inorganic Black Carbon over Kenya from 2019 to 2021.

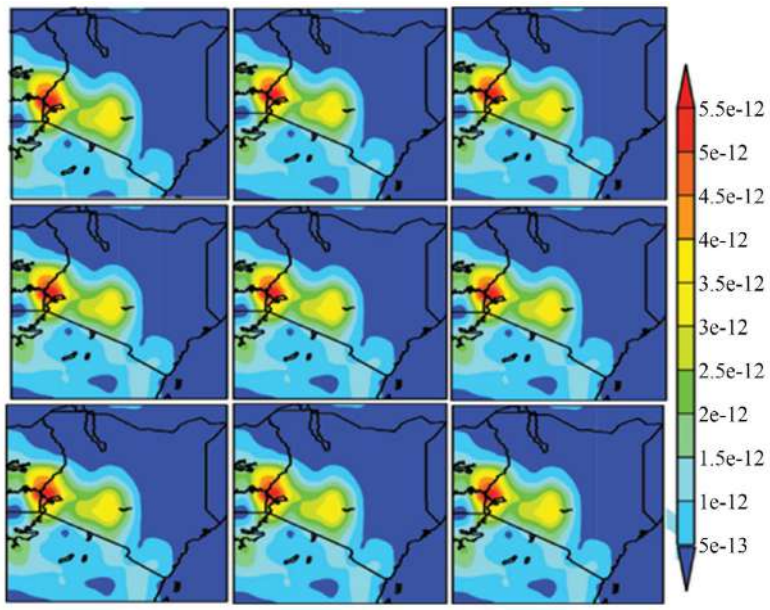

Figure 3. Spatial variability of BC over Kenya from 2019 to 2021.

It is also apparent from Figure 3 (Spatial maps of BC concentration over Kenya

in 2020) that the BC concentrations over Kenya do not show a significant reduction during the lockdown period but it points to the fact there was significant spatial variation in the emission of black carbon over Kenya. It is evident that the Western and the Rift Valley regions especially Nakuru County registered high concentrations of black carbon as opposed to the northern, northeastern and southwestern regions of the Kenya territory.

4.2. Sulphur Dioxide

The concentration of atmospheric SO_2 over Kenya is lower in the period April to July 2020 as depicted by the annual 24-hour average concentration time series in Figure 4. This trend is a result of the heavy downwash during this period. There is a high correlation between meteorological parameters, for instance pressure, precipitation, wind speed, temperature, relative humidity, and spatial concentration of SO_2 (Calkins et al., 2016). The average concentration of SO_2 for the years 2019-2020 and 2021 are 0.000189, 0.000197, and 0.000196 μgm^{-3}, respectively. However, the values of the concentration of SO_2 are far below the WHO guideline value of 20 µg. this is attributed to Kenya having fewer sources of SO_2 such as relatively less traffic since fossil fuel is the main source of SO_2 (Mutama et al., 2024).

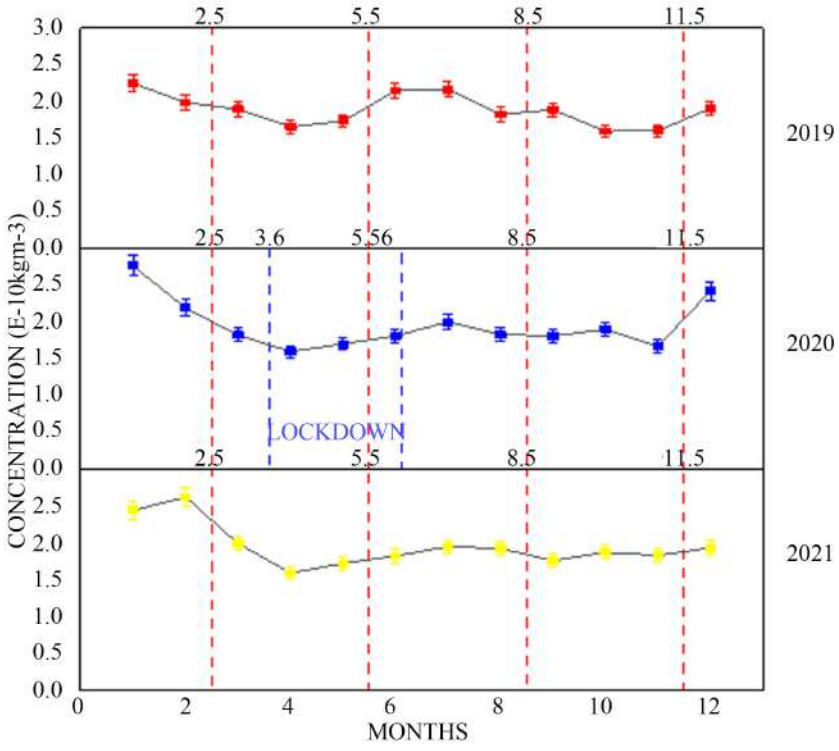

Figure 4. Time series, total Area-Average of surface mass concentration of SO_2 over Kenya from 2019 to 2021 daily concentration.

The spatial variation of the concentration of SO_2 is represented in Figure 5. The highest concentration of SO_2 is recorded at Mombasa City, followed by the Paka

region in Kerio Valley and parts of Malaba and Busia border points in Busia County.

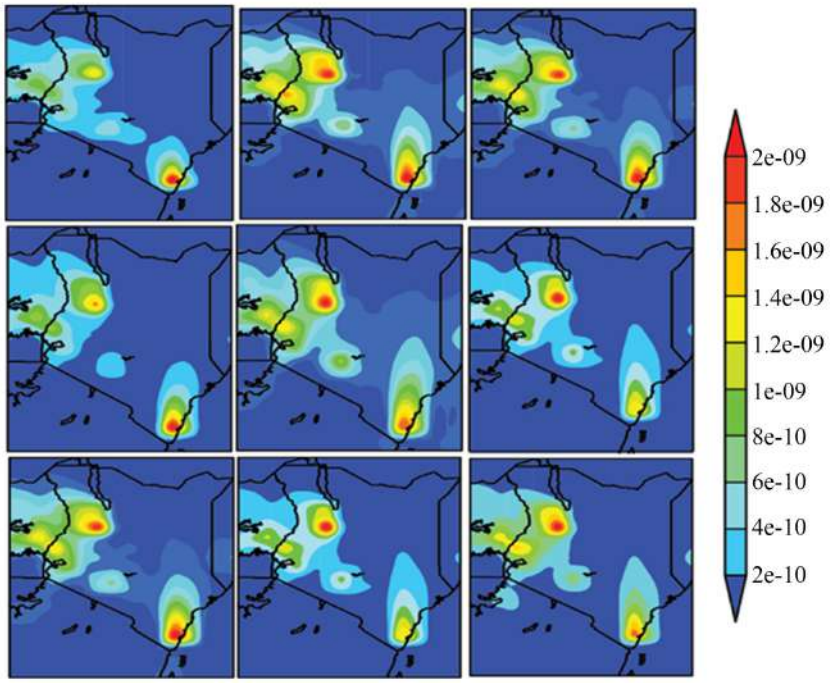

Figure 5. Spatial variability of SO_2 over Kenya from 2019 to 2021.

There is a statistically significant correlation between the SO_2 concentrations and the location of the main sources of SO_2 emissions. The high concentration of SO_2 around Mombasa is associated with the oil refinery, port activities, and the emission from transit trucks. The geothermal activity at the Paka area in Kerio Valley is a significant source of SO_2 in the region. SO_2 is mainly emitted from combustion of fossil fuels, through smelting of mineral ores and emissions from underground that contain Sulphur (Levelt et al., 2006; Lippi et al., 2012). However, the emission of SO_2 in parts of Busia County is associated with the busy highway linking Kenya to Uganda. The highway section between Bungoma and Tororo towns is a hotspot because of the slow flow of trucks and the limited effect of wind since the altitude and wind speed are relatively lower in this section. The spatial maps in **Figure 5** depict a situation where the regions around Mombasa, Nakuru, Paka in Kerio Valley, and Malaba are considered hotspots of high concentrations of SO_2. The scenario in Mombasa is associated with port activities in while emissions from the Olkaria Geothermal Power Station in Nakuru County contribute to high concentrations of SO_2 in the area. The emissions from hot springs in the Paka region of Kerio Valley (**Figure 5**) and emissions from truck and vehicle fleets along the Mombasa-Malaba highway are considered the main sources in these domains. Apart from being closer to the sources, the high concentration of SO_2 in these regions has a high correlation to lower wind velocity because of low altitude. However, there is no significant change in SO_2 concentration in

Kenya because of lockdowns. The highway section in areas with high altitudes and strong winds such as Eldoret, Nairobi, and parts of Makueni County register low concentrations of SO_2 because of strong winds/trajectories. Statistically, a significant association was not found between the concentration of atmospheric SO_2 to lockdowns and curfews instituted between March and June 2020. This is because of the lockdown, curfews, and COVID-19 protocols not being stringent in manufacturing, transit truck fleets, and industrial operations associated with SO_2 emissions.

4.3. Nitrogen Dioxide

Figure 6 demonstrates the spatial distribution of NO_2 surface concentration over Kenya during the 2019-2020 and 2020 months that correspond to the study period in 2020. Unlike other pollutants, NO_2 is almost exclusively sourced from anthropogenic activities. NO_2 is an unstable chemical and as a result, it makes it easy to convert to nitrate and form secondary aerosols. Therefore, the spatial distribution of NO_2 can directly reflect distribution and concentration of human activities (Saleem et al., 2024).

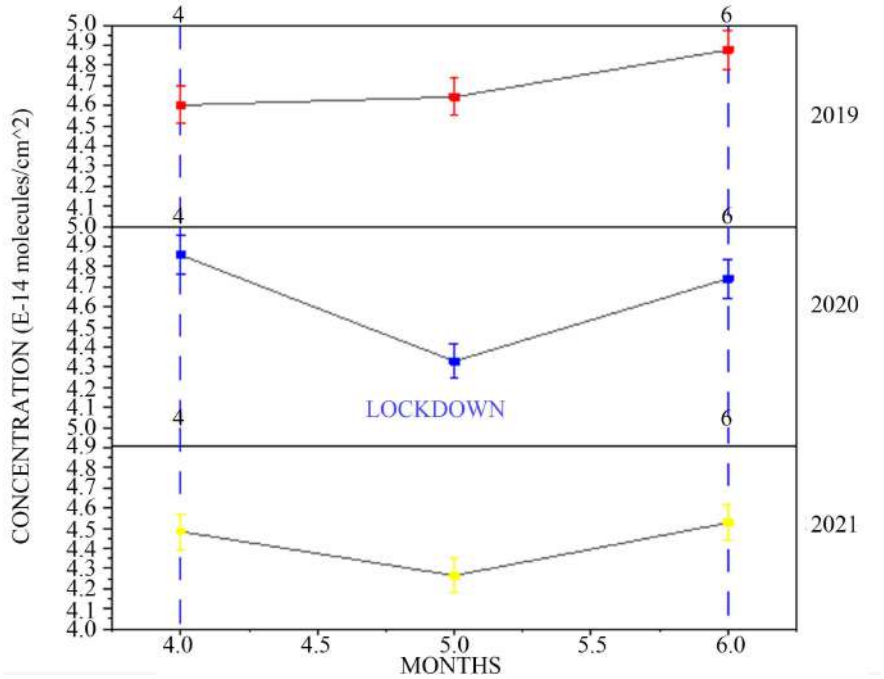

Figure 6. Time series, total area-average of surface mass concentration of NO_2 over Kenya from 2019 to 2021.

The concentration remains steady from March to June, after which a steady rise is noted, with concentration hitting $6.0 \times 10^{15}/cm^2$ in early June, a period that coincides with the end of the national lockdown.

The graph in Figure 6 depicts a relatively lower concentration of NO_2 in April to May within the year 2020 in comparison to the same months in the years 2019 to 2021. This is a result of limited anthropogenic activities during the lockdown

phase in 2020. The variation in emission NO_2 is lowest in comparison to the same months in the pre-lockdown and post-lockdown phases. From the spatial maps in Figure 7, the concentration of NO_2 is lowest in May 2020. The decline is associated with the reduction in work commutes, economic and industrial activities, and vehicle driving activity both locally and globally.

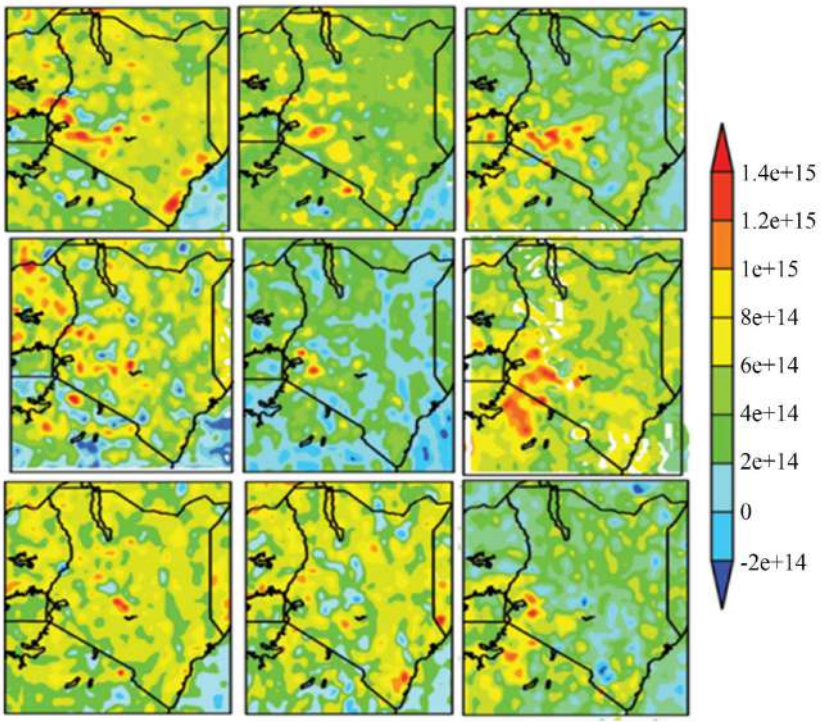

Figure 7. Spatial variability of NO_2 over Kenya from 2019 to 2021.

4.4. Ozone Gas

O_3 concentration has had an increasing trend from January to April 2020 as shown by the time series in Figure 8, however for the period that coincides with the COVID-19 lockdown in the year 2020 the level is seen to decline slightly after which it rises steadily. This is in contrast to other preceding and succeeding years (2019 and 2021). The cause of this increase was because of reduced NO which, consequently contributes to decline in the consumption of O_3 as depicted by the chemical equation $NO + O_3 = NO_2 + O_2$ and therefore causes an increase in the concentration of O_3. Interestingly, the total column concentration of O_3 noticeably increased during the lockdown period in the north and northeast parts of the country as depicted by Figure 9. The month of May 2020 registered the highest concentration of ozone gas total column as depicted by the spatial maps in Figure 8. The above scenario could be as a result of three possible reasons. First, the reduced concentration of nitrogen oxides (NO_x) because of the lockdown may lead to an O_3 concentration to shoot-up, deviating from the behavior during same period in the 2019 when there was no lockdown declared.

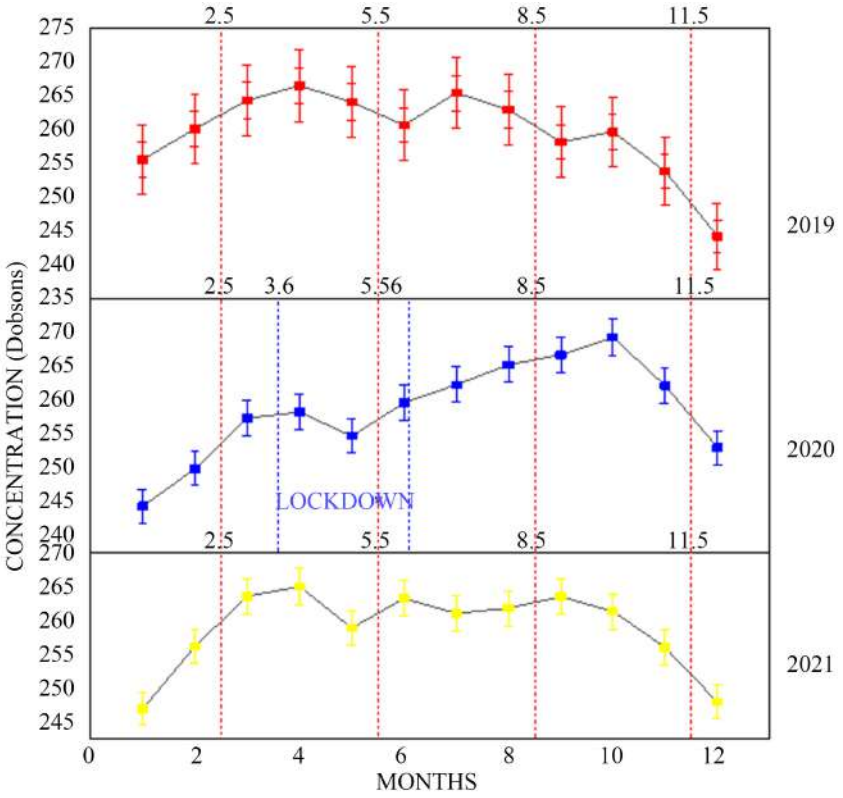

Figure 8. Time series, total area-average Ozone total column daily concentration 0.25 degrees over Kenya from 2019 to 2021.

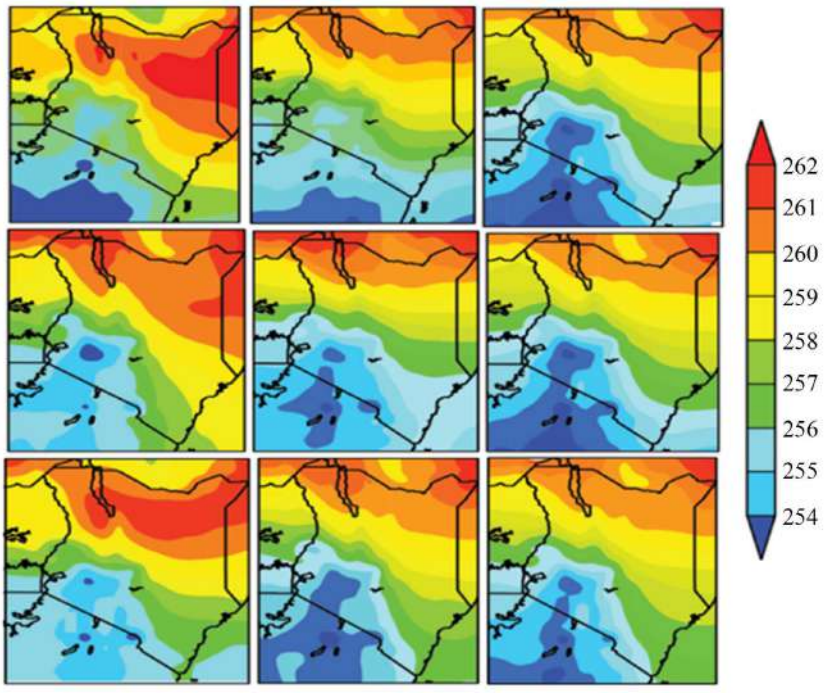

Figure 9. Spatial variability of O_3 over Kenya from 2019 to 2021.

Thirdly, due to the improvement in insolation and temperatures as a result of

the sun migrating to the equatorial region between March and June which contributes to increased concentration of O_3 (Songa, 2017). It is also apparent from the spatial maps in **Figure 9** that the region around Nakuru city had the lowest concentration of O_3 in the year 2020 as compared to other parts of the country.

This is because of the relatively higher NOx concentration as compared to the norm as a result of continuous emission from the Olkaria Geothermal Power Station and economic activity in the traditionally active agricultural south rift region despite the lockdowns.

4.5. Carbon Monoxide

The lifespan of CO in lower atmosphere has been estimated to range between 0.3 years and 5 years (Jaffe, 1968) and as a result the effect of reduction in concentration of CO during lockdown periods is only realized in the year succeeding the lockdown year as depicted by **Figure 10** and **Figure 11** respectively. It is postulated that several sinks for CO exists in the lower atmosphere (Jaffe, 1968). These include, the migration of accumulated CO from various sources due to atmospheric mixing, oxidation to carbon dioxide by atomic O_2 in the presence of ultraviolet radiation and oxidation and conversion by anaerobic methane -producing soil mechanisms in the presence of moisture. CO concentrations also reveal distinct seasonal patterns (Jaffe, 1968; Songa, 2017), with highest concentrations occurring during the windy (Songa, 2017) January, February months and the next highest concentrations occurring in the August, September months, mainly due to local meteorology, temperature inversions fluctuations in traffic modes and economic activities.

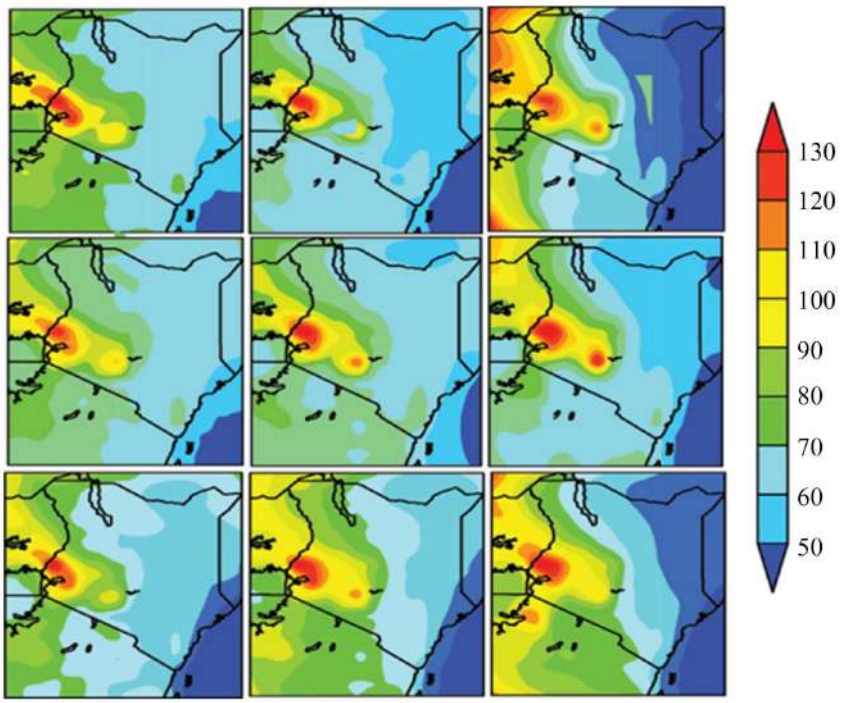

Figure 10. Spatial variability of CO over Kenya from 2019 to 2021.

The basic meteorological parameters that dictate the distribution of ozone gas include wind speed, wind direction, turbulence (Jaffe, 1968) and atmospheric chemistry. Counties in western Kenya, parts of the south rift valley around Nakuru account for the highest levels of concentration of CO as depicted by the spatial map in Figure 10. This fact is largely associated with emissions from large-scale biomass burning from farms and minimal contribution from traffic and industrial emissions. The concentrations are relatively higher in low altitude regions as a result of low wind speed.

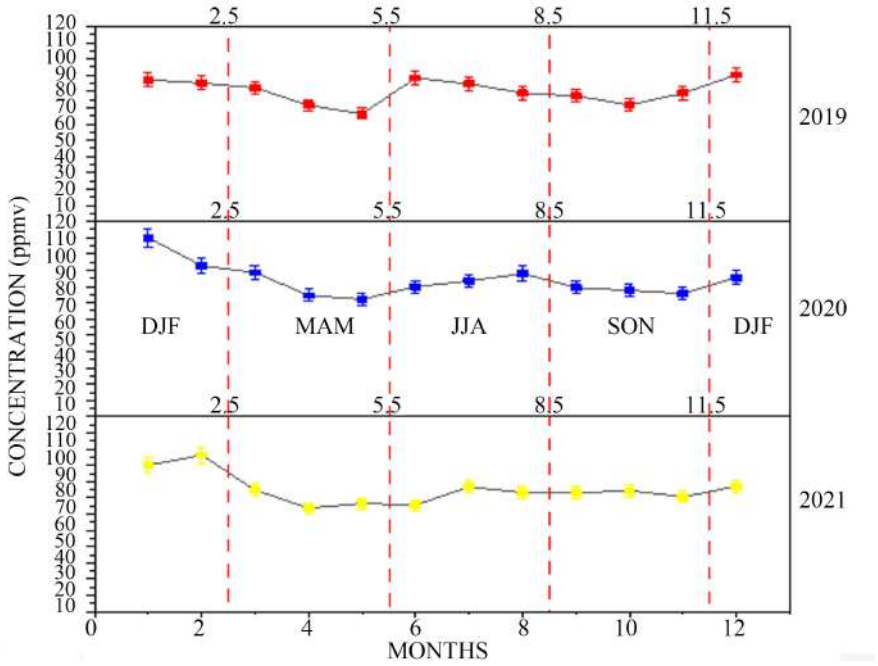

Figure 11. Time series, total area-average CO total column daily concentration 0.25 degrees over Kenya from 2019 to 2021.

4.6. Recommendations

The finding of this study gives an in-depth understanding of the distribution of sources of pollution, the extent and the factors that affect pollution levels over the Kenyan territory. It is therefore recommended that this knowledge be utilized in designing mitigation policies that will avert this situation. The analyzed data obtained should inform the establishment of an air impact assessment project with particular interest in identifying the pollution hotspots which will inform policy on approval of human settlements. The results on the state of air quality should inform the designing of an air quality index, a parameter that is key in assessing air quality, but Kenya does not have it in application. This is because reliance on other nation's air quality index to assess air quality will not give accurate measurement of air quality over Kenya since the extent of pollution levels differ as depicted by the findings of this research.

5. Conclusion

The territorial meteorology and anthropogenic factors have had a great influence

on the seasonality and diurnal variation of main pollutants in Kenya. The reduction of the concentration of NO_2 pollutants during lockdown months is registered primarily due to low economic activity and less traffic flow during that period; it slowly reduced and hit a minimum during the lockdown period. The concentration of BC and greenhouse gases did not register any decline during the study period. However, the time series for all the pollutants recorded an annual variation, registered because of meteorological factors such as rainfall, which cause a downwash of aerosols and temperatures that affect atmospheric chemistry. There is also the effect of migration of aerosols from other regions as depicted by backward trajectory analysis done in previous studies.

Authors' Declaration

We confirm that this research article is original work and has not been published previously by other journals except in the form of an abstract or as part of a published lecture or academic thesis.

Author's Contribution

Conceptualization: Peter M. Mutama, John W. Makokha, Festus B. Kelonye.

Methodology: Peter M. Mutama, John W. Makokha, Goeffrey W. Khamala.

Investigation: Peter M. Mutama, John W. Makokha, Festus B. Kelonye.

Discussion of Results: Peter M. Mutama, John W. Makokha, Goeffrey W. Khamala, Festus B. Kelonye.

Writing—Original Draft: Peter M. Mutama.

Writing—Review and Editing: Peter M. Mutama, John W. Makokha, Festus B. Kelonye.

Resources: John W. Makokha, Goeffrey W. Khamala.

Supervision: John W. Makokha, Festus B. Kelonye.

Approval of the final text: Peter M. Mutama, John W. Makokha, Festus B. Kelonye, Goeffrey W. Khamala.

Acknowledgements

As I blend the various bits of this article, it is my pleasure to express my appreciation to all the people and institutions that helped me during my entire master's study period. I would like to acknowledge too the contributions of Directorate of Geospatial technologies services, Vihiga County, for allowing me to learn GIS applications in their laboratories. I would like to thank the National Aeronautical Space Administration (NASA) for establishing the Moderate Resolution Imaging Spectroradiometer (MODIS) sensors, the Ozone Monitoring Instrument (OMI) sensors and the MERRA-2 models. I also thank the Giovanni Earth Data online platform which provided online data that forms the basis of my statistics in this study. Finally, by all supreme, I am indebted to God for granting me good health and insight.

Conflicts of Interest

The authors declare that there is no conflict of interest in the publication of this work.

References

Worldometer (2025). *Kenya Population (LIVE).* https://www.worldometers.info/world-population/kenya-population/

Arora, S., Bhaukhandi, K. D., & Mishra, P. K. (2020). Coronavirus Lockdown Helped the Environment to Bounce Back. *Science of the Total Environment, 742,* Article ID: 140573. https://doi.org/10.1016/j.scitotenv.2020.140573

Bai, H., Gao, W., Zhang, Y., & Wang, L. (2022). Assessment of Health Benefit of PM2.5 Reduction during COVID-19 Lockdown in China and Separating Contributions from Anthropogenic Emissions and Meteorology. *Journal of Environmental Sciences, 115,* 422-431. https://doi.org/10.1016/j.jes.2021.01.022

Boiyo, R., Kumar, K. R., Zhao, T., & Bao, Y. (2017). Climatological Analysis of Aerosol Optical Properties over East Africa Observed from Space-Borne Sensors during 2001-2015. *Atmospheric Environment, 152,* 298-313. https://doi.org/10.1016/j.atmosenv.2016.12.050

Calkins, C., Ge, C., Wang, J., Anderson, M., & Yang, K. (2016). Effects of Meteorological Conditions on Sulfur Dioxide Air Pollution in the North China Plain during Winters of 2006-2015. *Atmospheric Environment, 147,* 296-309. https://doi.org/10.1016/j.atmosenv.2016.10.005

Carslaw, D. (2005). Evidence of an Increasing NO/NO Emissions Ratio from Road Traffic Emissions. *Atmospheric Environment, 39,* 4793-4802. https://doi.org/10.1016/j.atmosenv.2005.06.023

Cheng, S., Ma, J., Zheng, X., Gu, M., Donner, S., Dörner, S. et al. (2021). Retrieval of O_3, NO_2, Bro and OCLO Columns from Ground-Based Zenith Scattered Light DOAS Measurements in Summer and Autumn over the Northern Tibetan Plateau. *Remote Sensing, 13,* Article 4242. https://doi.org/10.3390/rs13214242

De, D. K., Ikono, U. I., & Akinmeji, S. O. (2018). Health, Environmental Effects, the Control of Emission from Power Plants and the Need for a New Emission Capture Technology. *Journal of Physics: Conference Series, 1072,* Article ID: 012019. https://doi.org/10.1088/1742-6596/1072/1/012019

Ferranti, D. E., Benjamin, E. J., Blaha, M. J., Chiuve, S. E., Cushman, M., Das, S. R., Deo, R., Muntner, P. et al. (2017). Heart Disease and Stroke Statistics-2017 Update: A Report from the American Heart Association. *Circulation, 135,* e146-e603.

Gkatzelis, G. I., Gilman, J. B., Brown, S. S., Eskes, H., Gomes, A. R., Lange, A. C. et al. (2021). The Global Impacts of COVID-19 Lockdowns on Urban Air Pollution: A Critical Review and Recommendations. *Elementa: Science of the Anthropocene, 9,* Article ID: 00176. https://doi.org/10.1525/elementa.2021.00176

Gupta, M., Abdelmaksoud, A., Jafferany, M., Lotti, T., Sadoughifar, R., & Goldust, M. (2020). Covid-19 and Economy. *Dermatologic Therapy, 33,* e13329. https://doi.org/10.1111/dth.13329

Halmer, M. M., Schmincke, H., & Graf, H. (2002). The Annual Volcanic Gas Input into the Atmosphere, in Particular into the Stratosphere: A Global Data Set for the Past 100 Years. *Journal of Volcanology and Geothermal Research, 115,* 511-528. https://doi.org/10.1016/s0377-0273(01)00318-3

Hassan, M. A., Mehmood, T., Lodhi, E., Bilal, M., Dar, A. A., & Liu, J. (2022). Lockdown Amid COVID-19 Ascendancy over Ambient Particulate Matter Pollution Anomaly. *International Journal of Environmental Research and Public Health, 19,* Article 13540. https://doi.org/10.3390/ijerph192013540

Jaffe, L. S. (1968). Ambient Carbon Monoxide and Its Fate in the Atmosphere. *Journal of the Air Pollution Control Association, 18,* 534-540. https://doi.org/10.1080/00022470.1968.10469168

Karambu, M. C. H., Kigaru, D. M., & Ndung'u, Z. W. (2024). Parenting Approaches on Children Food Uptake and Nutrition Status in Kiambu County, Kenya. *International Journal of Advanced Research, 7,* 122-133. https://doi.org/10.37284/ijar.7.1.1822

Khadiagala, G. M. (2010). Boundaries in Eastern Africa. *Journal of Eastern African Studies, 4,* 266-278. https://doi.org/10.1080/17531055.2010.487337

Khamala, G. W., Makokha, J. W., Boiyo, R., & Kumar, K. R. (2022). Long-Term Climatology and Spatial Trends of Absorption, Scattering, and Total Aerosol Optical Depths over East Africa during 2001-2019. *Environmental Science and Pollution Research, 29,* 61283-61297. https://doi.org/10.1007/s11356-022-20022-6

Khan, R. R., & Siddiqui, M. J. (2014). Review on Effects of Particulates: Sulfur Dioxide and Nitrogen Dioxide on Human Health. *International Research Journal of Environmental Sciences, 3,* 70-73.

Kumar, A., Singh, P., Raizada, P., & Hussain, C. M. (2022). Impact of COVID-19 on Greenhouse Gases Emissions: A Critical Review. *Science of the Total Environment, 806,* Article ID: 150349. https://doi.org/10.1016/j.scitotenv.2021.150349

Kumar, N., Chu, A., & Foster, A. (2007). An Empirical Relationship between $PM_{2.5}$ and Aerosol Optical Depth in Delhi Metropolitan. *Atmospheric Environment, 41,* 4492-4503. https://doi.org/10.1016/j.atmosenv.2007.01.046

Kumar, S. (2017). Acid Rain-The Major Cause of Pollution: Its Causes, Effects. *International Journal of Applied Chemistry, 13,* 53-58.

Laurent, B., Marticorena, B., Bergametti, G., Léon, J. F., & Mahowald, N. M. (2008). Modeling Mineral Dust Emissions from the Sahara Desert Using New Surface Properties and Soil Database. *Journal of Geophysical Research: Atmospheres, 113,* D14218. https://doi.org/10.1029/2007jd009484

Levelt, P. F., Joiner, J., Tamminen, J., Veefkind, J. P., Bhartia, P. K., Stein Zweers, D. C. et al. (2018). The Ozone Monitoring Instrument: Overview of 14 Years in Space. *Atmospheric Chemistry and Physics, 18,* 5699-5745. https://doi.org/10.5194/acp-18-5699-2018

Levelt, P. F., van den Oord, G. H. J., Dobber, M. R., Malkki, A., Huib Visser,, Johan de Vries, et al. (2006). The Ozone Monitoring Instrument. *IEEE Transactions on Geoscience and Remote Sensing, 44,* 1093-1101. https://doi.org/10.1109/tgrs.2006.872333

Li, R. R., Kaufman, Y. J., Mattoo, S., Remer, L. A., Chu, D. A., Martins, J. V., Tanre, D. et al. (2003). The MODIS Aerosol Algorithm, Products and Validation.

Lippi, G., Rastelli, G., Meschi, T., Borghi, L., & Cervellin, G. (2012). Pathophysiology, Clinics, Diagnosis and Treatment of Heart Involvement in Carbon Monoxide Poisoning. *Clinical Biochemistry, 45,* 1278-1285. https://doi.org/10.1016/j.clinbiochem.2012.06.004

Lukiw, W. J., Pogue, A., & Hill, J. M. (2022). SARS-CoV-2 Infectivity and Neurological Targets in the Brain. *Cellular and Molecular Neurobiology, 42,* 217-224. https://doi.org/10.1007/s10571-020-00947-7

Mahato, S., Pal, S., & Ghosh, K. G. (2020). Effect of Lockdown Amid COVID-19 Pandemic

on Air Quality of the Megacity Delhi, India. *Science of the Total Environment, 730,* Article ID: 139086. https://doi.org/10.1016/j.scitotenv.2020.139086

Makokha, J. W., Odhiambo, J. O., & Godfrey, J. S. (2017). Trend Analysis of Aerosol Optical Depth and Ångström Exponent Anomaly over East Africa. *Atmospheric and Climate Sciences, 7,* 588-603. https://doi.org/10.4236/acs.2017.74043

Meng, X., Ma, Y., Chen, R., Zhou, Z., Chen, B., & Kan, H. (2013). Size-Fractionated Particle Number Concentrations and Daily Mortality in a Chinese City. *Environmental Health Perspectives, 121,* 1174-1178. https://doi.org/10.1289/ehp.1206398

Misiani, Z., Lun, Y., Niu, S., Lü, J., & Zhang, L. (2019). A GIS Based Approach to Back Trajectory Analysis and Mass Concentration & Dispositions of Aerosols in Nairobi, Kenya. *Journal of Geoscience and Environment Protection, 7,* 122-139. https://doi.org/10.4236/gep.2019.72009

Monsen, K. A. (2024). *Intervention Effectiveness Research: Quality Improvement and Program Evaluation in Healthcare: A Practical Guide to Real-World Implementation.* Springer.

Mutama, P. M., Makokha, J. W., Kelonye, F. B., & Khamala, G. W. (2024). Spatial-Temporal Assessment of Changes in Aerosol Optical Properties Pre, During, and Post COVID-19 Lockdowns over Kenya, East Africa. *Open Access Library Journal, 11,* 1-14. https://doi.org/10.4236/oalib.1111223

Ndolo, I. J. (2018). *Effects of Urbanization on Rainfall and Temperature over the City of Nairobi, Kenya.* Master's Thesis, University of Nairobi.

Obiero, J. P. O., & Onyando, J. O. (2013). Climate. *Developments in Earth Surface Processes, 16,* 39-50. https://doi.org/10.1016/b978-0-444-59559-1.00005-0

Otmani, A., Benchrif, A., Tahri, M., Bounakhla, M., Chakir, E. M., El Bouch, M. et al. (2020). Impact of Covid-19 Lockdown on PM_{10}, SO_2 and NO_2 Concentrations in Salé City (Morocco). *Science of the Total Environment, 735,* Article ID: 139541. https://doi.org/10.1016/j.scitotenv.2020.139541

Pant, P., & Harrison, R. M. (2013). Estimation of the Contribution of Road Traffic Emissions to Particulate Matter Concentrations from Field Measurements: A Review. *Atmospheric Environment, 77,* 78-97. https://doi.org/10.1016/j.atmosenv.2013.04.028

Remer, L. A., Kaufman, Y. J., Tanré, D., Mattoo, S., Chu, D. A., Martins, J. V. et al. (2005). The MODIS Aerosol Algorithm, Products, and Validation. *Journal of the Atmospheric Sciences, 62,* 947-973. https://doi.org/10.1175/jas3385.1

Saleem, F., Hina, S., Ullah, I., Habib, A., Hina, A., Ilyas, S. et al. (2024). Impacts of Irregular and Strategic Lockdown on Air Quality over Indo-Pak Subcontinent: Pre-To-Post COVID-19 Analysis. *Chaos, Solitons & Fractals, 178,* Article ID: 114255. https://doi.org/10.1016/j.chaos.2023.114255

Songa, C. M. M. (2017). *Modeling the Solar Forcing of the Total Column Ozone Variation in Selected Cities in Kenya.* Master's Thesis, COPAS, JKUAT.

Venter, Z. S., Aunan, K., Chowdhury, S., & Lelieveld, J. (2020). COVID-19 Lockdowns Cause Global Air Pollution Declines. *Proceedings of the National Academy of Sciences of the United States of America, 117,* 18984-18990. https://doi.org/10.1073/pnas.2006853117

Wong, M. S., Zhu, R., Yin Tung Kwok, C., Kwan, M., Santi, P., Ho Liu, C. et al. (2021). Association between No_2 Concentrations and Spatial Configuration: A Study of the Impacts of COVID-19 Lockdowns in 54 US Cities. *Environmental Research Letters, 16,* Article ID: 054064. https://doi.org/10.1088/1748-9326/abf396

World Health Organization (2006). *World Health Organization Air Quality Guidelines for Particulate Matter, Ozone, Nitrogen Dioxide and Sulphur Dioxide: Global Update 2005: Summary of Risk Assessment* (pp. 1-22). World Health Organization.

World Health Organization (2020). *Infection Prevention and Control during Health Care When Novel Coronavirus (nCoV) Infection Is Suspected Interim Guidance, 19 March 2020.*